This article has been accepted for publication in IEEE Antennas and Wireless Propagation Letters. This is the author's version which has not been fully edited and content may change prior to final publication. Citation information: DOI 10.1109/LAWP.2021.3124075

Compact Hybrid Metasurface-Inspired Resonator with Uniform Magnetic Field Distribution for Wireless Power Transfer

Pavel Smirnov, Polina Kapitanova, Elizaveta Nenasheva, and Mingzhao Song

***Abstract*—Compact and safe charging platforms have been one of the main goals in wireless power transfer (WPT) research and development. Here we propose a compact hybrid metasurface-inspired resonator with a uniform magnetic field distribution for WPT. It consists of two orthogonally oriented layers of parallel printed wires with high-permittivity dielectric pads between them. This design allows to spatially separate electric and magnetic fields, which provide high WPT efficiency and electromagnetic safety simultaneously. The prototype with 28 cm $\times$ 28 cm working area with uniform magnetic field was fabricated and experimentally studied. The measured coefficient of variation of the magnetic field in the working area of the resonator is 6.8%. The maximum achievable WPT efficiency reaches 70% over the working area. The numerically assessed specific absorption rate in human tissues placed on the proposed structure is 11 mW/kg, which is 30 times lower than on a conventional planar spiral coil. Our results pave the way to compact and safe WPT platforms for one-to-many charging.**

***Index Terms*—Wireless power transfer, metasurface, near magnetic field, resonator.**

I. Introduction

With the advent of the 5G era and the rapid rise of applications such as the Internet of Things, a large number of electronic devices have different requirements for electric energy in various scenarios, which has given birth to a convenient power supply fashion. Wireless power transfer (WPT) has become a key technology that needs to be developed urgently today [1], [2]. Among various WPT technologies, magnetic resonant power transfer (MRPT) [3], [4], which aims to enlarge transfer distance and increase power transfer efficiency, is considered to be one of the most promising WPT technology in the future. MRPT systems usually use two resonant coils to transmit and receive the energy. To obtain high WPT efficiency, they should have the same size and be located coaxially at a certain distance for operation in a critical coupling regime. However, any deviation from these conditions leads to a crucial drop in WPT efficiency.

Nowadays, an increased number of personal electronic devices require regular and frequent charging, which has led to the emergence of a new direction of WPT, i.e. one-to-many WPT [5]–[8]. In this concept, the transmitting resonator should be large enough to accommodate several small receivers (Rx), and the WPT efficiency is desired to be stable wherever the Rx is placed on the transmitter (Tx). It was shown that MRPT systems have the potential to implement this concept [9], but the conventional coil resonators need to be modified to meet the following two requirements. First, the magnetic fields should be uniformly distributed on the Tx in order to solve the problem of Rx misalignment. Second, the electric field leakage must be well confined to guarantee human safety around a large working area over the Tx.

The uniform magnetic field distribution can be obtained in multiple ways. In [10]–[15] different Txs were proposed to generate uniform magnetic fields. However, these structures have a number of disadvantages, such as complex coil or complicated power scheme designs [10], [11], discrepancy of the magnetic field [12], small working area compared to the coil size [13], etc. Also, all of the structures are based on planar spiral coil (PSC) designs which do not confine the electric field which limits its maximal allowable operation power. Therefore these designs are hard to be applied in consumer mobile-oriented WPT scenarios.

Recently, metasurface-inspired resonators have been proposed for WPT [12], [16], [17]. Some of them can be classified as hybrid structures consisting of resonant metallic units and high permittivity material decorations for the manipulation of magnetic and electric fields, respectively. For instance, hybrid resonators with a large area and uniform magnetic field distribution can be made from a wire-array structure [16], [18]. High permittivity microwave materials such as distilled water can be used as a surrounding background to confine the electric field [17]. However, WPT Tx with compactness, uniform fields and low specific absorption rate (SAR) being achieved simultaneously have not been reported so far.

In this letter, we propose a hybrid metasurface-inspired transmitting resonator for WPT systems. We numerically study the eigenmodes of the structure and parametric dependencies

The work was supported by Natural Science Foundation of China (Project No. 62101154), Natural Science Foundation of Heilongjiang Province of China (Project No. LH2021F013), Fundamental Research Funds for the Central Universities (Project No. 3072021CFJ0802), Research Funds for the Key Laboratory of Advanced Marine Communication and Information Technology of the Ministry of Industry and Information Technology (Project No. AMCIT21V2), and Russian Science Foundation (Project No. 20-72-10090). *(Corresponding author: Mingzhao Song.)*

Pavel Smirnov and Polina Kapitanova are with the Department of Physics and Engineering, ITMO University, 197101, Saint Petersburg, Russia (e-mail: pavel.smirnov@metalab.ifmo.ru; p.kapitanova@metalab.ifmo.ru).

Elizaveta Nenasheva is with Ceramics Co., Ltd, 194223, Saint Petersburg, Russia.

Mingzhao Song is with the College of Information and Communication Engineering, Harbin Engineering University, 150001, Harbin, China, Key Laboratory of Advanced Marine Communication and Information Technology, Ministry of Industry and Information Technology, Harbin Engineering University, Harbin, China, and also with Department of Physics and Engineering, ITMO University, 197101, Saint Petersburg, Russia (e-mail: kevinsmz@foxmail.com).

This article has been accepted for publication in IEEE Antennas and Wireless Propagation Letters. This is the author's version which has not been fully edited and content may change prior to final publication. Citation information: DOI 10.1109/LAWP.2021.3124075

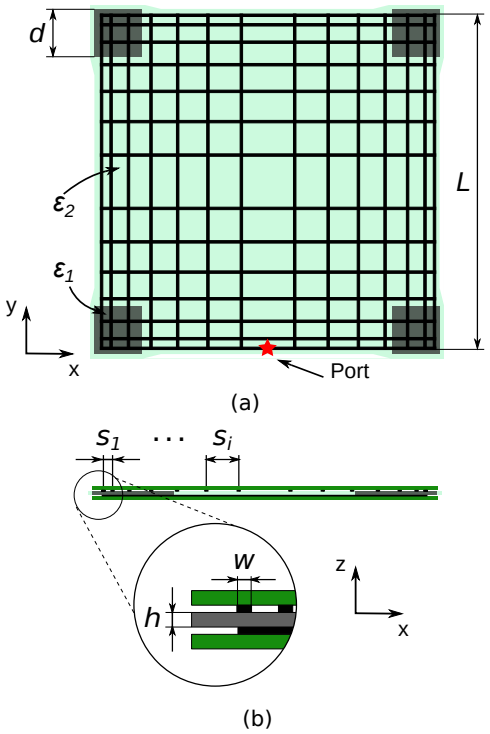

Fig. 1. Configuration of the hybrid metasurface-inspired resonator: (a) top view, and (b) side view with a close-up edge shown in the inset.

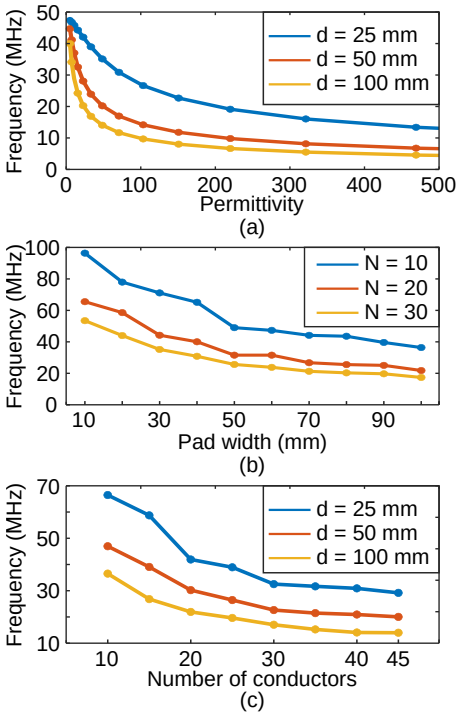

Fig. 2. The fundamental mode frequency dependence as a function of (a) permittivity of dielectric pads, (b) size of dielectric pads, (c) number of wires in each layer.

of their frequencies, optimize the geometry to obtain high uniformity of the magnetic field in a large area and also demonstrate the reduced SAR in comparison to conventional (PSC) and other Tx designs. We fabricate and experimentally study the prototype of the hybrid metasurface-inspired resonator to support numerical results.

II. Resonator Design and Analysis

A. Configuration and Operation Principle

Crossing-wire resonator was reported in [17], which shows good electric field shielding, but has a cumbersome profile and non-uniform magnetic field distribution. To improve manufacturability and WPT performance we propose a new compact hybrid metasurface-inspired resonator configuration, shown in Fig. 1. It consists of two orthogonally oriented layers of parallel printed metallic wires of length L and width w. Wires are distributed with a subwavelength spacing s_i. In the corners of the structure, square dielectric pads with width d, thickness h and permittivity ε_1 are inserted. The rest part between the layers is filled with low-index ($\varepsilon_2 \ll \varepsilon_1$) material for mechanical supporting.

The hybrid metasurface resonator based on wire-array supports a series of eigenmodes of the structure [19], [20], which is due to a strong coupling between two units with subwavelength spacing. When the second wire layer is added, capacitive coupling occurs between layers, which can be further enhanced by high permittivity dielectric insertions in the corners. Excitation of the structure induces a current in wires which form a set of nested current loops and creates a vertically oriented magnetic field [17]. The presence of the second layer allows to spatially separate magnetic and electric fields in the near-field region [17]. The high permittivity dielectric insertions also increase the capacitive load of wires and decrease the eigenmode frequencies, which can be used for operation frequency tuning. In this way, the electric field is confined between two layers, whereas the magnetic field is distributed around the whole structure and the resonant frequency is decreased.

B. Eigenmode Analysis

Initially, the wire structure with equidistant wire distribution was considered and mode analysis was performed in CST Microwave Studio 2020 to define the mode with the uniform magnetic field distribution. For a fixed resonator size (L = 38 cm, w = 2 mm, h = 2 mm) the influence of the following parameters on the eigenmode frequency was investigated: the size of dielectric pads, the dielectric permittivity, and the number of wires. It was observed that a uniform magnetic field over the resonator was created on the fundamental mode, while the higher-order modes have magnetic field hot-spots distributed to the edges. Here, we consider the fundamental mode as the operational one, because it can potentially provide a high WPT efficiency regardless of the Rx position. The resulting parametric dependencies for the fundamental mode are presented in Fig. 2. It can be seen that the achievable working frequency of the hybrid resonator can be adjusted in a wide range (5-100 MHz) for a fixed length of wires, and the biggest impact on flexibility results from the permittivity of dielectric pads. Almost the whole permittivity range from

This article has been accepted for publication in IEEE Antennas and Wireless Propagation Letters. This is the author's version which has not been fully edited and content may change prior to final publication. Citation information: DOI 10.1109/LAWP.2021.3124075

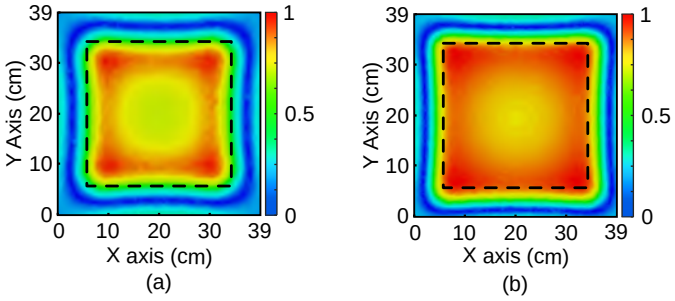

Fig. 3. Z-component of the magnetic field at a plane 30 mm above the hybrid resonator with (a) equidistant wire distribution, and (b) optimizes wire distribution. Here the fields are normalized to the maximal field intensity of 9 A/m for the equidistant case and 7.8 A/m for the optimized one.

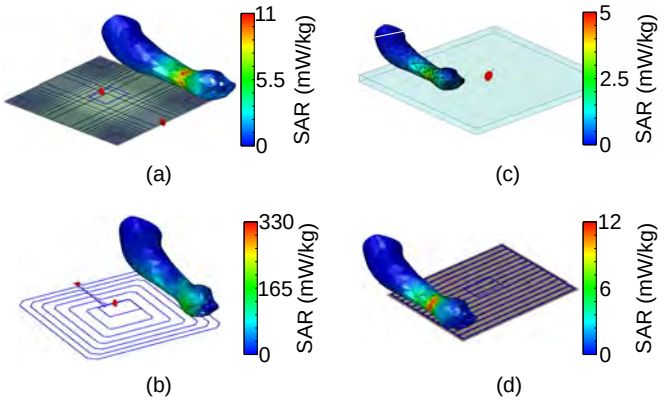

Fig. 4. The SAR of different transmitters of WPT systems: (a) hybrid resonator, (b) PSC with 38 cm × 38 cm size, (c) crossing-wire resonator [17], (d) capacitor-loaded wires resonator [16]. For all structures the following simulation condition were used: matched Rx was placed in the center and the human forearm model was located above the region of highest electric field (worst case) at the height z = 15 mm above Tx.

Fig. 2(a) can be covered by composite ceramic materials which also have a low loss at high frequencies [21]–[23].

C. Magnetic Field Optimisation

Further simulations were performed by the frequency domain solver of CST Microwave Studio 2020. The resonator is excited with a port inserted in the slit in the center of the lateral wire as shown in Fig. 1(a) with the red star. Based on parametric analysis in the previous section, the operational frequency of 27 MHz was tuned using the following parameters: L = 38 cm, w = 2 mm, h = 2 mm, d = 80 mm, N = 30, ε = 55. The normalized magnetic field distribution at the working frequency at the 30 mm plane above the resonator is shown in Fig. 3(a). A reduction of magnetic field strength in the center can be observed, which is due to wire arrangement of the resonator. To quantify this non-uniformity of the field we introduced the coefficient of variation (COV) defined as the ratio of the standard deviation of the magnetic field to its mean value [15]. For the structure with equidistant wire distribution, the calculated COV is 15.2% in the working area 28 cm × 28 cm which is shown in Fig. 3(a) by a dashed line.

To increase the uniformity of the field in the working area the number of wires of the resonator and spacing between them was optimized. Part of the wires in the center N_1 = 10 was distributed according to the law from [15] with spacing s_i determined as: $s_i = L(f_i - f_{i+1})$, where f_i is a ratio between the i-th wire counting from the edge of the structure to the length of the wire, which is defined as $f_i = (1-(N-i+1)/N)^k$, where N is the total number of wires, i is the order number of wire, counting from the edge, k = 0.28 is the optimized coefficient of non-uniformity. The peripheral wires N_2 = 24 were kept equidistantly distributed with spacing s = 7.5 mm. The fundamental mode frequency was tuned to 27 MHz by the size and permittivity of the dielectric inserts (d = 54 mm, ε = 45). The optimized magnetic field distribution is shown in Fig. 3(b). One can see that the magnetic field became more uniform in the working area. The calculated COV is 6.6%, which is 2.3 times lower than the non-optimised case.

D. SAR Assessment

SAR is commonly used for a quantitative assessment of the human exposure to the electromagnetic field, which is defined as: $SAR = \sigma |E|^2 / 2\rho$, where σ is conductivity of the tissue, E is the electric field strength and ρ is the density of the tissue [24]. To assess the SAR of the hybrid resonator we considered a typical application scenario of WPT systems: energy is transferred to a matched Rx, and a human hand is located near the Tx. The result of SAR calculation for human forearm model [25] for 1 W input power is shown in Fig. 4(a). The peak SAR value is 11 mW/kg, and the peak electric field near the forearm is 260 V/m. International standards limit the maximum value of SAR to 4 W/kg in the limbs [26], [27]. Accordingly, up to 350 W of power could be transmitted without significant harm to a human.

We also performed a comparison of the proposed structure with conventional PSC and metasurface-based resonators [16], [17], shown in Fig. 4(b-d). As can be seen from Fig. 4(b), the SAR of a PSC is an order of magnitude higher than the SAR of a hybrid resonator which is 330 mW/kg. Therefore, its use for high-power applications might pose a serious danger to people and other biological objects that are nearby the WPT system. The SAR of the crossing-wire resonator [17] is twice lower than the SAR of the proposed hybrid resonator, as shown in Fig. 4(c). This follows from the fact that a crossing-wire resonator is immersed in a high permittivity host medium, which makes it possible to concentrate electric field inside and reduce the SAR. In comparison, a relatively low SAR can be still obtained in a compact profile of the proposed resonator.

III. Experimental Investigation and Comparison

A prototype of the optimized hybrid resonator was fabricated and measured. Its photograph is shown in Fig. 5(a). The wires were made by means of PCB technology on a 1 mm thick FR-4 substrate (ε = 4.3, tanδ = 0.025). Dielectric pads were manufactured from $CaTiO_3$-based ceramic (ε = 45, tanδ = 0.0005) [21]. To excite the structure, SMA connector was mounted in a 5 mm slit of the lateral wire. To ensure the mechanical strength of the structure, fix the pads and ensure a constant height between the layers over the entire area of the resonator, the holder was made using additive printing

This article has been accepted for publication in IEEE Antennas and Wireless Propagation Letters. This is the author's version which has not been fully edited and content may change prior to final publication. Citation information: DOI 10.1109/LAWP.2021.3124075

TABLE I
COMPARISON OF VARIOUS WPT TRANSMITTERS

Ref.	Frequency (MHz)	Working area (cm × cm)	COV (%)	Efficiency (%)	SAR (mW/kg)
[11]	13.56	20 × 20	12	–	–
[12]	13.56	22 × 22	–	60	–
[16]	17	21 × 31	23	80	12
[17]	36	35 × 35	37	70	4.6
PSC	27	28 × 28	25	77	330
This work	27	28 × 28	6.8	70	11

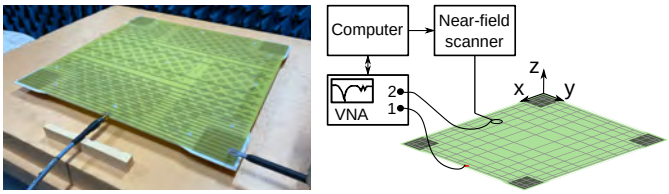

Fig. 5. (a) Photograph and (b) the experimental setup of the hybrid metasurface-inspired resonator prototype.

technology from ABS plastic (ε = 2.8, tanδ = 0.03) [28]. All parts were fixed together with polyamide fasteners.

The measurement setup is shown in Fig. 5(b). To measure the near magnetic field distribution the resonator was connected to the first port of a vector network analyzer (VNA) Rohde & Schwarz ZVB 20. The Langer EMV-Technic XF-R 100 magnetic field probe was connected to the second port of VNA and placed in parallel plane to the resonator at z = 30 mm to measure the normal component of the magnetic field. It was moved along the plane using a high-precision 3D positioner (near-field scanner) [29] with 0.5 cm step and complex value of the transmission coefficient was measured at each point. From this data the distribution of magnetic field was extracted and is shown in Fig. 6(a). The measured field distribution is in a good agreement with the simulated one from 3(b). We also show the normalized amplitudes of the magnetic field along the dashed diagonal line both for equidistant and optimized wire distribution in Fig. 6(b). The simulated and measured field profiles coincide well and have higher field strength in the center in comparison to the equidistant wire distribution case. The measured value of COV in the working area is 6.8%.

To measure the efficiency a simple WPT system was realized. The hybrid resonator acted as a Tx and a single-loop coil sized 9 cm × 6 cm acted as an Rx. Both of them were connected to the VNA to measure the S-parameters of the system herewith the separation between Tx and Rx was 15 mm, and the scanning of the working area was done with a 1 cm step. The maximum available WPT efficiency (i.e. the ratio of the power in the load to the power available from the source when the Tx is matched with the source and the load is optimized to maximize the efficiency) was extracted using measured S-parameters [30], [31]. The result is presented in Fig. 7(a). The efficiency reaches 70% and is almost constant in the working area regardless of Rx position. The dependence of the COV and efficiency to the Rx located at the center of the resonator from the height above it was also studied and the

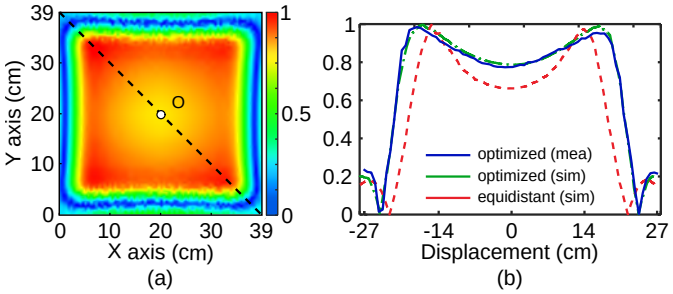

Fig. 6. (a) Measured normalized z-component magnetic field distribution at a plane 30 mm above the resonator. (b) Comparison of measured and simulated normalized to the maximum z-component of the magnetic field along the diagonal dashed line for the hybrid resonator with optimized wire distribution and the simulated case with equidistant distribution.

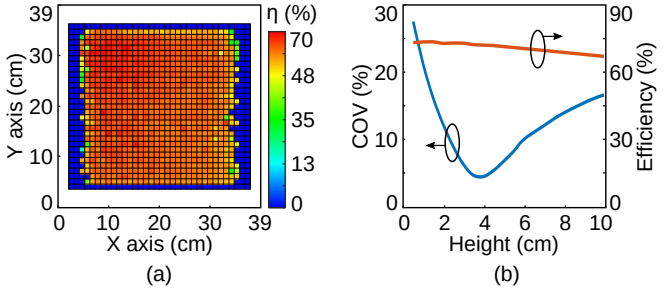

Fig. 7. (a) Measured maximum available efficiency to a single-loop receiver, (b) dependence of efficiency and COV from the height above Tx.

result is shown in Fig. 7(b). The efficiency slightly decreases as the height increases, while the COV has a minimum near the desired working plane.

In the Table I we compare the performance of the proposed hybrid resonator with a classical PSC and previously reported WPT Txs with uniform magnetic field. For [16], [17] and PSC the working area was defined as half of the whole area of the Tx. The main advantage of the hybrid metasurface-inspired resonator is the lowest COV in the working area. Also, it has 30 times lower SAR in comparison with a PSC of the same size. However, hybrid resonator does not show the best WPT efficiency performance. One may conclude that the proposed hybrid resonator is a compromise between large working area with low COV, efficiency and SAR, which pave the way to its application in safe and efficient one-to-many WPT systems.

IV. CONCLUSION

The hybrid metasurface-inspired resonator has been proposed and studied both numerically and experimentally. The eigenmode parametric analysis shows that the fundamental mode has a uniform magnetic field profile and its resonant frequency can be adjusted in the 5-100 MHz range for the fixed resonator size (38 cm × 38 cm). By optimizing the wire distribution, a highly uniform magnetic field has been obtained with the measured COV of 6.8% in the working area. The measured WPT efficiency also reaches 70% in a large area regardless of the Rx position. It was also shown that the proposed structure has a peak SAR value 11 mW/kg which is 30 times lower than a PSC with the same size, and thereby it can increase the exposure safety of WPT systems.

REFERENCES

[1] M. Song, P. Jayathurathnage, E. Zanganeh, M. Krasikova, P. Smirnov, P. Belov, P. Kapitanova, C. Simovski, S. Tretyakov, and A. Krasnok, "Wireless power transfer based on novel physical concepts," *Nature Electronics*, vol. 4, no. 10, pp. 707–716, 2021.

[2] M. Song, P. Belov, and P. Kapitanova, "Wireless power transfer inspired by the modern trends in electromagnetics," *Applied Physics Reviews*, vol. 4, no. 2, 2017.

[3] A. Kurs, A. Karalis, R. Moffatt, J. D. Joannopoulos, P. Fisher, and M. Soljačić, "Wireless power transfer via strongly coupled magnetic resonances," *Science*, vol. 317, no. 5834, pp. 83–86, 2007.

[4] X. Wei, Z. Wang, and H. Dai, "A critical review of wireless power transfer via strongly coupled magnetic resonances," *Energies*, vol. 7, no. 7, pp. 4316–4341, 2014.

[5] J. Song, M. Liu, and C. Ma, "Analysis and design of a high-efficiency 6.78-MHz wireless power transfer system with scalable number of receivers," *IEEE Transactions on Industrial Electronics*, vol. 67, no. 10, pp. 8281–8291, 2020.

[6] W. Liu, K. Chau, C. Lee, C. Jiang, W. Han, and W. Lam, "Multi-Frequency Multi-Power One-to-Many Wireless Power Transfer System," *IEEE Transactions on Magnetics*, vol. 55, no. 7, 2019.

[7] Z. Dai, Z. Fang, H. Huang, Y. He, and J. Wang, "Selective Omnidirectional Magnetic Resonant Coupling Wireless Power Transfer With Multiple-Receiver System," *IEEE Access*, vol. 6, pp. 19 287–19 294, 2018.

[8] Y. J. Kim, D. Ha, W. J. Chappell, and P. P. Irazoqui, "Selective Wireless Power Transfer for Smart Power Distribution in a Miniature-Sized Multiple-Receiver System," *IEEE Transactions on Industrial Electronics*, vol. 63, no. 3, pp. 1853–1862, 2016.

[9] B. L. Cannon, J. F. Hoburg, D. D. Stancil, and S. C. Goldstein, "Magnetic Resonant Coupling As a Potential Means for Wireless Power Transfer to Multiple Small Receivers," *IEEE Transactions on Power Electronics*, vol. 24, no. 7, pp. 1819–1825, 2009.

[10] C. Cai, J. Wang, H. Nie, P. Zhang, Z. Lin, and Y. G. Zhou, "Effective-Configuration WPT Systems for Drones Charging Area Extension Featuring Quasi-Uniform Magnetic Coupling," *IEEE Transactions on Transportation Electrification*, vol. 6, no. 3, pp. 920–934, 2020.

[11] Q. Xu, Q. Hu, H. Wang, Z. H. Mao, and M. Sun, "Optimal Design of Planar Spiral Coil for Uniform Magnetic Field to Wirelessly Power Position-Free Targets," *IEEE Transactions on Magnetics*, vol. 57, no. 2, 2021.

[12] F. S. Sandoval, S. M. Delgado, A. Moazenzadeh, and U. Wallrabe, "A 2-D magnetoinductive wave device for freer wireless power transfer," *IEEE Transactions on Power Electronics*, vol. 34, no. 11, pp. 10 433–10 445, 2019.

[13] Y. Zhang, L. Wang, Y. Guo, and Y. Zhang, "Optimisation of planar rectangular coil achieving uniform magnetic field distribution for EV wireless charging based on genetic algorithm," *IET Power Electronics*, vol. 12, no. 10, pp. 2706–2712, aug 2019. [Online]. Available: https://onlinelibrary.wiley.com/doi/10.1049/iet-pel.2018.6202

[14] X. Liu and S. Y. Hui, "Optimal design of a hybrid winding structure for planar contactless battery charging platform," *IEEE Transactions on Power Electronics*, vol. 23, no. 1, pp. 455–463, 2008.

[15] J. J. Casanova, Z. Ning Low, J. Lin, and R. Tseng, "Transmitting coil achieving uniform magnetic field distribution for planar wireless power transfer system," in *2009 IEEE Radio and Wireless Symposium*, 2009, pp. 530–533.

[16] M. Song, P. Smirnov, E. Puhtina, E. Zanganeh, S. Glybovski, P. Belov, and P. Kapitanova, "Multi-mode metamaterial-inspired resonator for near-field wireless power transfer," *Applied Physics Letters*, vol. 117, no. 8, p. 083501, aug 2020. [Online]. Available: http://aip.scitation.org/doi/10.1063/5.0012006

[17] A. Markvart, M. Song, S. Glybovski, P. Belov, C. Simovski, and P. Kapitanova, "Metasurface for Near-Field Wireless Power Transfer with Reduced Electric Field Leakage," *IEEE Access*, vol. 8, pp. 40 224–40 231, 2020.

[18] A. V. Shchelokova, A. P. Slobozhanyuk, I. V. Melchakova, S. B. Glybovski, A. G. Webb, Y. S. Kivshar, and P. A. Belov, "Locally Enhanced Image Quality with Tunable Hybrid Metasurfaces," *Physical Review Applied*, vol. 9, no. 1, p. 014020, 2018.

[19] F. Lemoult, G. Lerosey, J. De Rosny, and M. Fink, "Resonant metalenses for breaking the diffraction barrier," *Physical Review Letters*, vol. 104, no. 20, pp. 1–4, 2010.

[20] F. Lemoult, M. Fink, and G. Lerosey, "Revisiting the wire medium: An ideal resonant metalens," *Waves in Random and Complex Media*, vol. 21, no. 4, pp. 591–613, 2011.

[21] E. A. Nenasheva, L. P. Mudroliubova, and N. F. Kartenko, "Microwave dielectric properties of ceramics based on CaTiO3-LnMO3 System (Ln-La, Nd; M-Al, Ga)," *Journal of the European Ceramic Society*, vol. 23, no. 14, pp. 2443–2448, 2003.

[22] E. A. Nenasheva, N. F. Kartenko, I. M. Gaidamaka, O. N. Trubitsyna, S. S. Redozubov, A. I. Dedyk, and A. D. Kanareykin, "Low loss microwave ferroelectric ceramics for high power tunable devices," *Journal of the European Ceramic Society*, vol. 30, no. 2, pp. 395–400, 2010.

[23] E. A. Nenasheva, S. S. Redozubov, N. F. Kartenko, and I. M. Gaidamaka, "Microwave dielectric properties and structure of ZnO-Nb2O5-TiO2 ceramics," *Journal of the European Ceramic Society*, vol. 31, no. 6, pp. 1097–1102, 2011.

[24] K. Guido and A. Kiourti, "Wireless Wearables and Implants: A Dosimetry Review," *Bioelectromagnetics*, vol. 41, no. 1, pp. 3–20, 2020.

[25] H. Tankaria, X. J. Jackson, R. Borwankar, G. N. Srichandhru, A. Le Tran, J. Yanamadala, G. M. Noetscher, A. Nazarian, S. Louie, and S. N. Makarov, "VHP-Female full-body human CAD model for cross-platform FEM simulations - Recent development and validations," *Proceedings of the Annual International Conference of the IEEE Engineering in Medicine and Biology Society, EMBS*, vol. 2016-October, pp. 2232–2235, 2016.

[26] *IEEE Std C95.1™-2019 IEEE Standard for Safety Levels With Respect to Human Exposure to Radio Frequency Electromagnetic Fields, 3 kHz to 300 GHz*. New York: IEEE, 2019.

[27] "Guidelines for limiting exposure to time-varying electric, magnetic, and electromagnetic fields (up to 300 GHz). International Commission on Non-Ionizing Radiation Protection," *Health Physics*, vol. 74, no. 4, pp. 494–522, 1998. [Online]. Available: http://www.icnirp.org/cms/upload/publications/ICNIRPemfgdl.pdf

[28] B. Riddle, J. Baker-Jarvis, and J. Krupka, "Complex permittivity measurements of common plastics over variable temperatures," *IEEE Transactions on Microwave Theory and Techniques*, vol. 51, no. 3, pp. 727–733, 2003.

[29] K. Haelvoet, S. Criel, F. Dobbelaere, L. Martens, P. De Langhe, and R. De Smedt, "Near-field scanner for the accurate characterization of electromagnetic fields in the close vicinity of electronic devices and systems," *Conference Record - IEEE Instrumentation and Measurement Technology Conference*, vol. 2, pp. 1119–1123, 1996.

[30] S. J. Orfanidis, *Electromagnetic Waves and Antennas*, 2016. [Online]. Available: https://www.ece.rutgers.edu/∼orfanidi/ewa/

[31] T. Ohira, "Maximum available efficiency formulation based on a black-box model of linear two-port power transfer systems," *IEICE Electronics Express*, vol. 11, no. 13, pp. 1–6, 2014.